Arabian Journal of Chemistry (2013) 6, 131–144

King Saud University

Arabian Journal of Chemistry

www.ksu.edu.sa
www.sciencedirect.com

ORIGINAL ARTICLE

Multiclass analysis on repaglinide, flubendazole, robenidine hydrochloride and danofloxacin drugs

Taleb T. Al-Nahary [a,*], Mohamed Abdel Nabi El-Ries [b,*], Gehad G. Mohamed [c], Ali Kamal Attia [b], Yahia Nasser Mabkhot [d], Michelyne Haroun [e], Assem Barakat [d]

[a] *Department of Chemistry, Faculty of Applied Science, Thamar University, P.O. Box 87246, Yemen*
[b] *National Organization for Drug Control and Research, 6-Abu Hazem St., Pyramide, P.O. Box 29, Cairo, Egypt*
[c] *Chemistry Department, Faculty of Science, Cairo University, P.O. Box 12613, Giza, Egypt*
[d] *Department of Chemistry, Faculty of Science, King Saud University, P.O. Box 2455, Riyadh 11451, Saudi Arabia*
[e] *Department of Pharmaceutical, College of Pharmacy, Umm Al-Qura University, Makkah, Saudi Arabia*

Received 18 June 2011; accepted 31 January 2012
Available online 8 February 2012

KEYWORDS

Repag;
Flu;
Roben and Dano;
EI-MS spectrometry;
Thermal analyses;
Molecular orbital calculation (MOC)

Abstract The drugs under study; repaglinide (Repag), flubendazole (Flu), robenidine hydrochloride (Roben) and danofloxacin (Dano) are antidiabetic, anthelmintic, anticoccidial, and antibiotic drugs. In the present study, they are investigated using electron impact mass spectral (EI-MS) fragmentation at 70 eV, in comparison with thermal analyses measurements (TGA/DrTGA and DTA) and molecular orbital calculation (MO). Semi-empirical MO calculation, AM1 procedure, has been carried out on Repag, Flu, Roben and Dano both as neutral molecules (in TA) and the corresponding positively charged species (in MS). The calculated MO parameters include bond length, bond order, charge distribution on different atoms and heat of formation. The fragmentation pathways of Repag, Flu, Roben and Dano in EI-MS led to the formation of important primary and secondary fragment ions. The mechanism of formation of some important daughter ions can be illuminated from comparing with that obtained using mass spectrometer through the accurate mass measurement determination. The MO provides a base for fine distinction among sites of initial bond cleavage and subsequent fragmentation of drug molecules in both thermal analysis and MS techniques. The activation thermodynamic parameters, such as, (activation energy E^*), (enthalpy

* Corresponding authors.
E-mail addresses: alnaharyt@yahoo.com (T.T. Al-Nahary), mohamedelries@hotmail.com (M.A.N. El-Ries).

Peer review under responsibility of King Saud University.
doi:10.1016/j.arabjc.2012.01.012

Production and hosting by Elsevier

ΔH^*), (entropy ΔS^*) and (Gibbs free energy ΔG^*) are calculated from the DrTGA curves using Coats–Redfern and Horowitz–Mitzger methods.

1. Introduction

Mass spectrometry plays a vital role in the structural characterization of biological molecules (Larsen and Me Ewen, 1998). The technique is important because it provides a lot of structural information with little expenditure of the sample. Also, the techniques offer comparative advantages for speed and productivity for pharmaceutical analysis (Kerns et al., 1997). On the other hand, thermal analysis technique that delivers extremely sensitive measurements of heat change can be applied on a broad scale with pharmaceutical development. These methods provide unique information relating to thermodynamic data of the system studied. The increasing use of the combined techniques is providing more specific information, and thus facilities more rapid interpretation of the experimental curves obtained (Zayed et al., 2007). In electron impact (EI) mass spectral fragmentation consists of competitive and consecutive unimolecular fragmentation pathways (Leversen, 1978). The fragmentation of ionized molecule depends mainly on their internal energy. The thermogravimetric TG/DTG analysis had been used to provide quantitative information on weight losses due to the decomposition and/or evaporation of low molecular materials as a function of temperature. In conjunction with mass spectrometric analysis (Fahmey et al., 2005), the nature of the released volatilized fragments may be deduced, thus greatly facilitating the interpretation of thermal degradation processes. On the other hand, computational quantum chemistry can provide additional information about atoms and bonds, which can be used successfully in an interpretation of experimental results (Somogyi et al., 1991). These additional computational data also, can be used in the description and prediction of primary fragmentation site and subsequent ones.

The aim of the present work is to make a correlation between mass spectral (MS) fragmentation and thermal analyses (TA) degradation of Repag, Flu, Roben and Dano drugs, then these data are compared with theoretical MO calculation to identify the weakest bonds ruptured during both mass and thermal studies. Consequently the choice of the correct pathway of such fragmentation knowing this structural session of bonds can be used to decide the active sites of this drug responsible for its chemical, biological and medical reactivities. Coats–Redfern and Horowitz–Mitzger methods were applied for calculating different thermodynamic functions accompanying the decomposition process of the drugs under investigation (Coats and Redfern, 1964; Horowitz and Metzegar, 1963).

2. Experimental

2.1. Mass spectrometry (MS)

Electron impact (EI) mass spectra of Repag, Flu, Roben and Dano drugs were obtained using Shimadzu-GC–MS-QP 1000 EX quadruple mass spectrometer with an electron multiplier detector equipped with the GC–MS data system (Fig. 1).

2.2. Thermal analyses (TA)

The thermal analyses of Repag, Flu, Roben and Dano drugs were made using Shimadzu thermogravimetric analyzer TGA-60H in a dynamic nitrogen atmosphere. Highly sintered α-Al_2O_3 was used as a reference. The mass losses of samples and heat response of the change of the sample were measured from room temperature up to 1000 °C. The heating rate was 10 °C min^{-1}.

2.3. Molecular orbital calculations (MO)

The MO calculations were performed using semi-emperical MO-calculation. The program used in these computations is hyperchem 7.5 by using AM1 method described by Dewar (Bourcier et al., 2003; Dewar et al., 1985; Zayed et al., 2007).

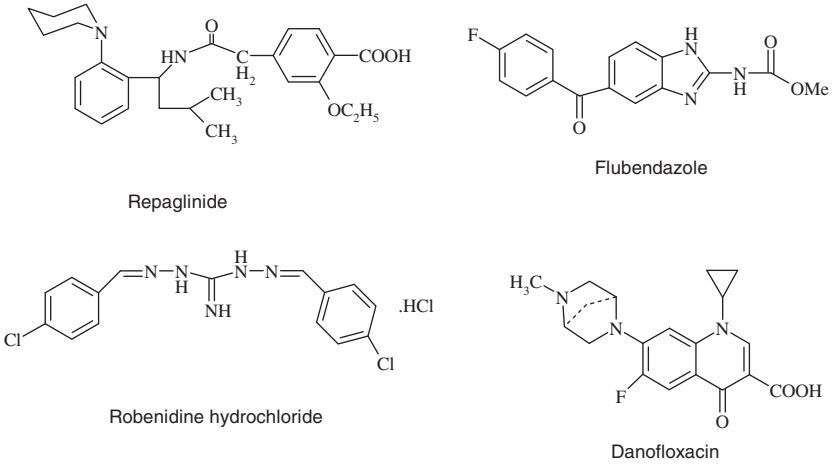

Figure 1 The molecular structures of the investigated drugs.

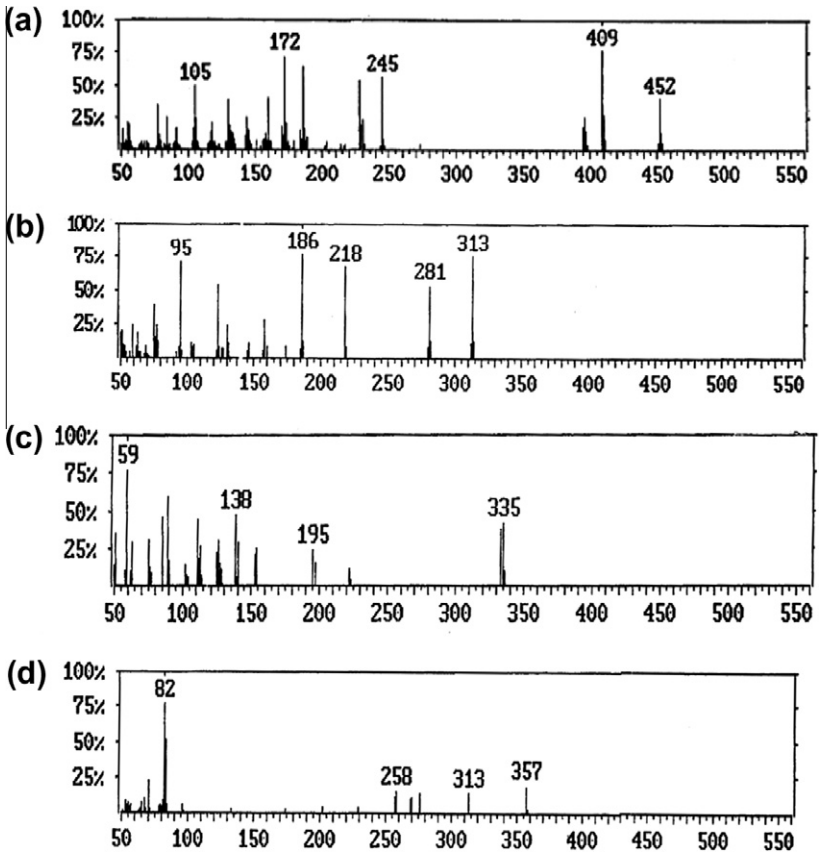

Figure 2 The mass spectra of (a) Repag, (b) Flu, (c) Roben and (d) Dano drugs.

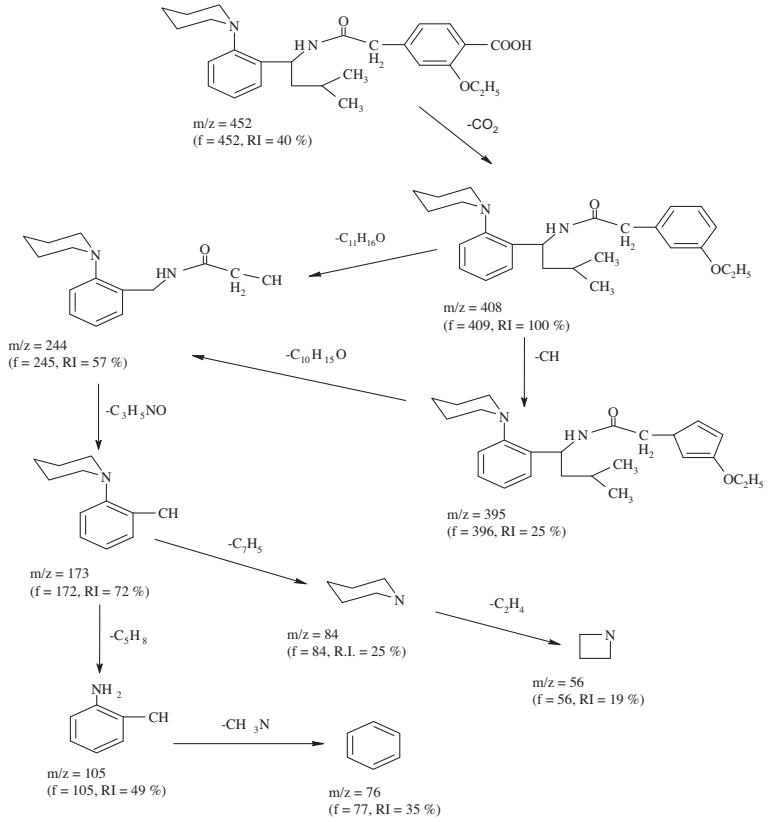

Scheme 1 Mass fragmentation pattern of Repag.

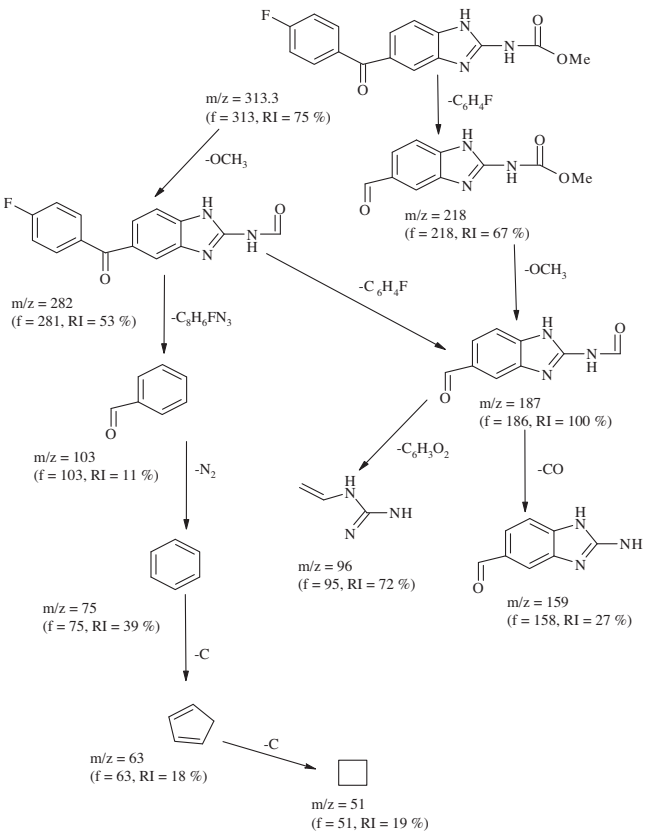

Scheme 2 Mass fragmentation pattern of Flu.

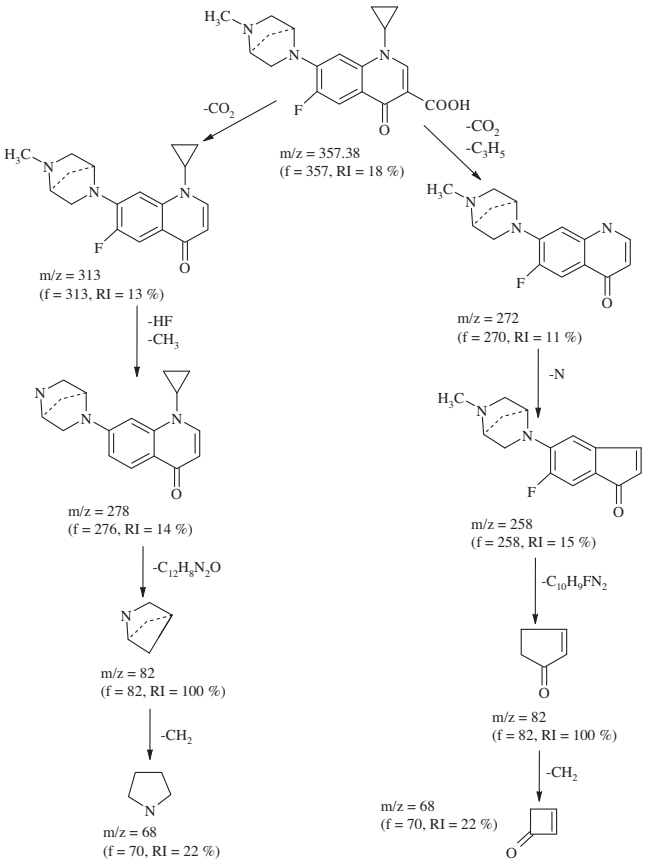

Scheme 4 Mass fragmentation pattern of Dano.

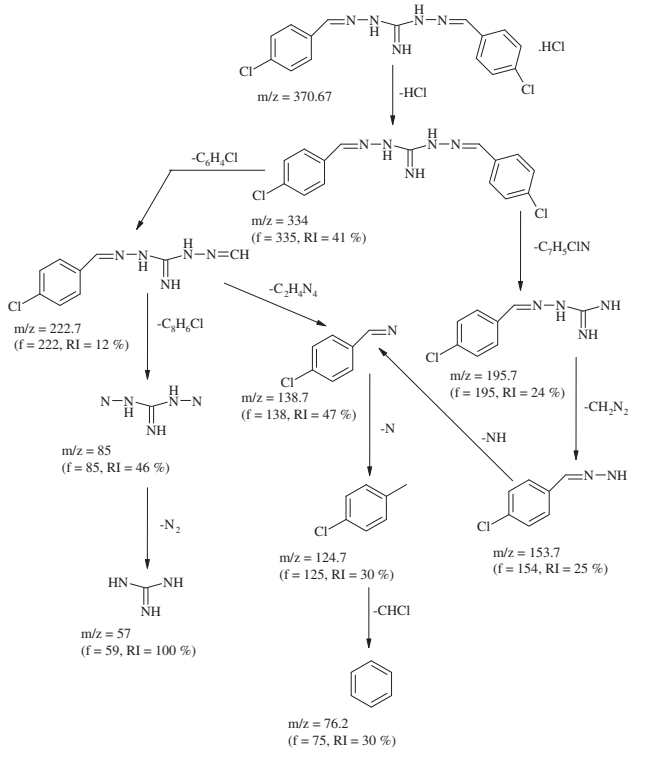

Scheme 3 Mass fragmentation pattern of Roben.

3. Results and discussion

It is of great interest to study the chemistry and reactivity of Repag, Flu, Roben and Dano drugs because of their importance in medicine knowledge. This knowledge can be obtained from thermal decomposition mechanism of the neutral drugs, which is very important to understand the chemical processes that charged in biological systems. It is difficult to establish the exact major fragmentation pathway in EI using conventional MS. Combining the two above techniques and the data obtained from the MO, it is possible to understand the following topics:

1. The stability of the drug under thermal degradation in solid state and mass spectral fragmentation in gas phase.
2. Prediction of the primary site of the fragmentation, which helps to rationalize subsequent bond cleavage.
3. The correct pathway in both techniques.

3.1. Mass spectra of Repag, Flu, Roben, and Dano

The mass spectra of the drugs are presented graphically in Fig. 2a–d. The different pathways of the possible fragments of Repag, Flu, Roben and Dano with their respective relative intensities (RI) are given in Schemes 1–4. Fragments at m/z = 409, 186, 59 and 82 (RI = 100%) represent the base peaks of Repag, Flu, roben and Dano, respectively. The other

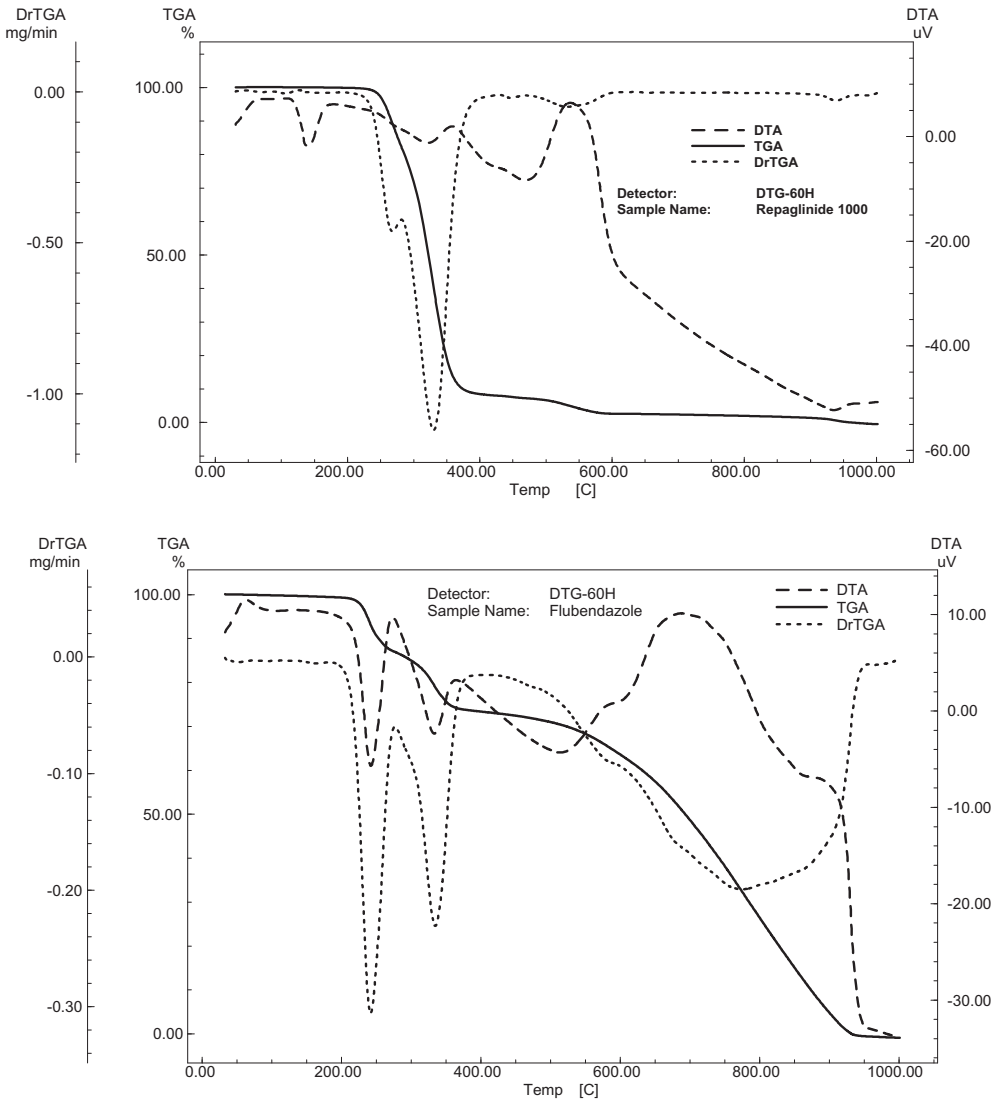

Figure 3 TGA, DrTGA and DTA curves of (a) Repag, (b) Flu, (c) Roban and (d) Dano drugs.

molecular ion peaks that appeared in the mass spectra are attributed to the fragmentation of the used drug molecules obtained from the rupture of different bonds inside the molecules.

3.2. Thermal analyses (TA) of Repag, Flu, Roben and Dano drugs

The thermal analyses data (TGA, DrTGA and DTA) of the drugs under investigation are shown in (Fig. 3). Table 1 summarizes that the weight losses occur in Repag, Flu, Roben and Dano drugs, and DTA; physical and chemical changes occur during thermal degradation of the drug neutral molecules. The study of the thermal decomposition of these drugs may give a good idea about the possible metabolites obtained during the biological assimilation in in vivo systems during their medical uses; consequently throws more light on their biological and medical activities. The TGA curves show that Repag, Flu, Roben and Dano molecules are thermally decomposed in three to four stages. The first stage occurs at 150–280, 100–275, 40–260 and 50–160 °C as a result of 17.0%, 14.66%, 9.79%% and 4.08% estimated weight losses which may be due to the loss of CO_2 and C_2H_6, CO_2, HCl, and CH_3 molecules (calcd. wt. loss = 16.37%, 14.06%, 9.85%, and 4.20%) for Repag, Flu, Roben and Dano molecules, respectively. The second stage occurs at 280–390, 275–380, 260–380, and 160–400 °C as a result of 74.25%, 13.53%, 59.93% and 35.35% estimated weight losses which may be due to the loss of $C_{22}H_{28}N_2O$, $CHNCH_3$, $C_9H_8N_5Cl$ and C_6H_6NO and HF molecules (calcd. wt. loss = 74.34%, 13.42%, 59.76%, and 35.82%) for Repag, Flu, Roben and Dano molecules, respectively. The third stage occurs within the temperature range from 390–1000, 380–950, 3870–800 and 400–500 °C with estimated weight losses of 9.40%, 27.31%, 31.02% and 12.35% which may be attributed to the complete decomposition of Repag, Flu and Roben and the loss of CO2 in the case of Dano (calcd. wt. loss = 9.29%, 72.31%, 30.35% and 12.31%). The third stage occurs in two successive steps in the case of Repag and Roben. The fourth stage occurs at 500–850 °C as a result of 48.25% estimated weight loss which may be due to the complete decomposition

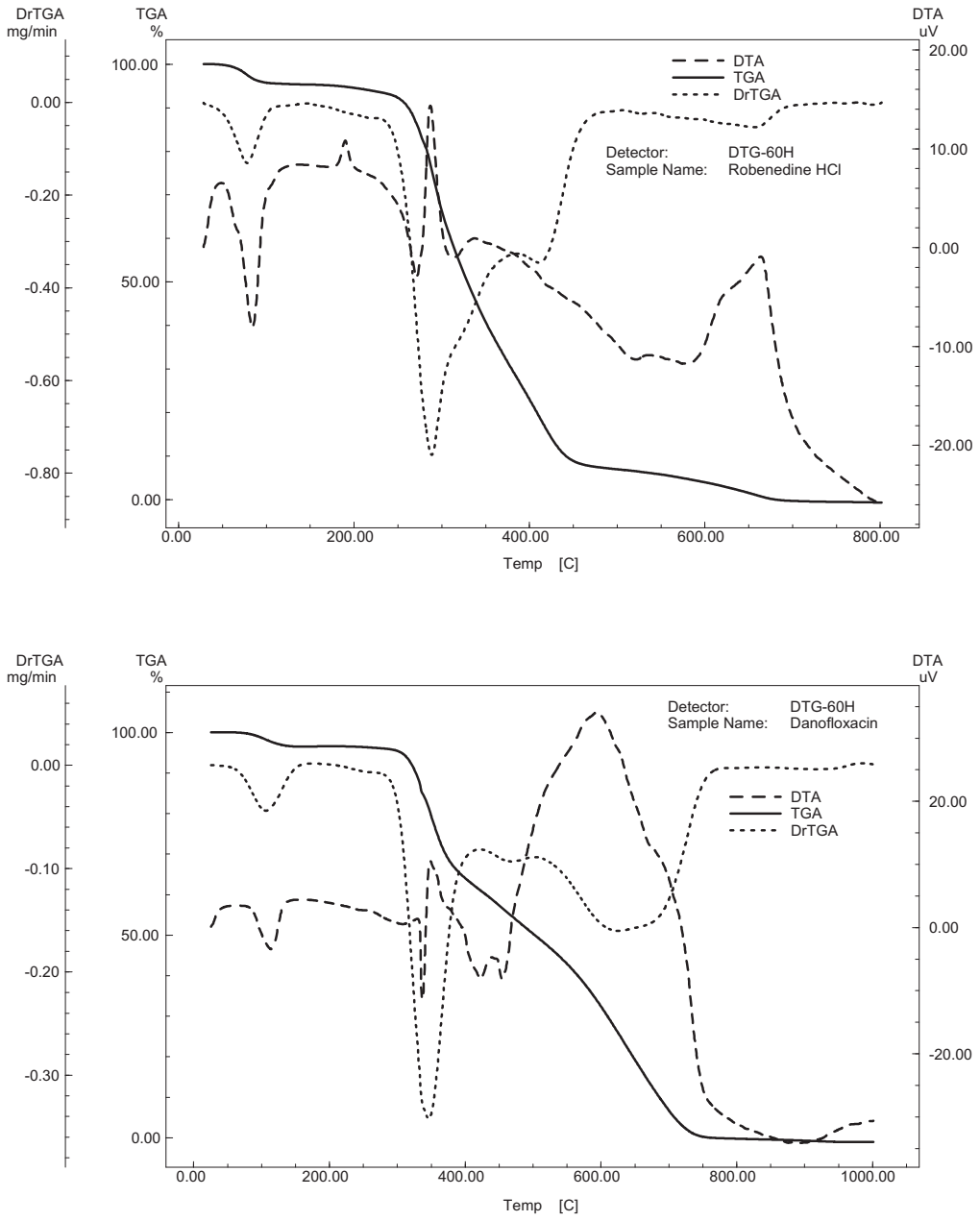

Figure 3 (*continued*)

Table 1 The relative abundance of Repag, Flu, Roben, and Dano fragments in their mass spectra.

Repag		Flu		Roben		Dano	
m/*z*	RI %	*m*/*z*	RI %	*m*/*z*	RI %	*m*/*z*	RI %
452	40	313	75	335	41	357	18
409	100	281	53	222	12	313	13
396	25	218	67	195	24	276	14
245	57	186	100	154	25	270	11
172	72	158	27	138	47	258	15
105	49	95	72	125	30	82	100
84	25	75	39	85	46	70	22
77	35	63	18	59	100	–	–
56	19	51	19	75	30	–	–

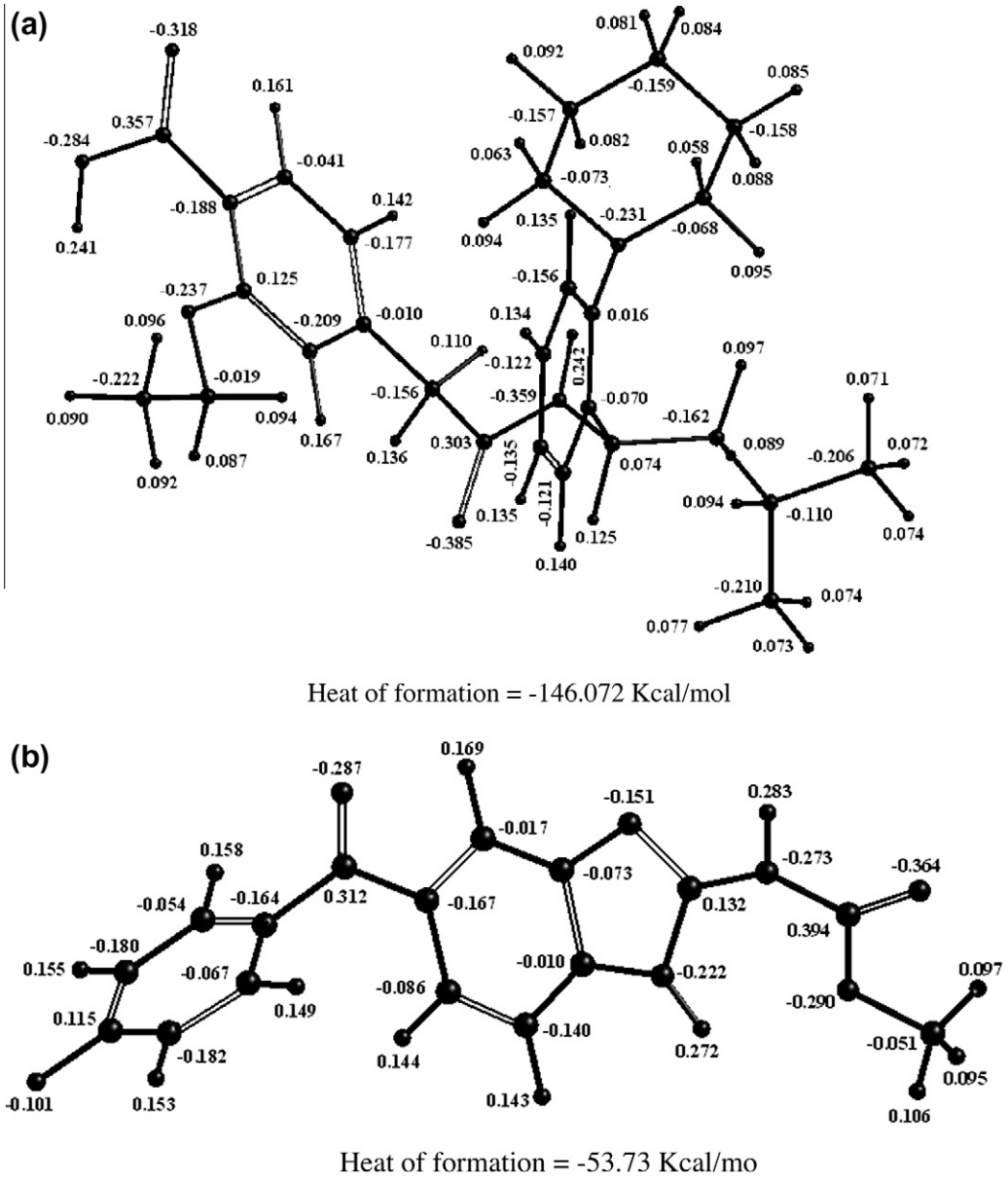

Figure 4 Charge distribution on different atoms for (a) Repag, (b) Flu, (c) Roben and (d) Dano neutral molecules.

of Dano (calcd. wt. loss = 47.57%). The weight losses appeared in DTA as strong endothermic and strong exothermic peaks as given by the data listed in Table 1 and shown in Fig. 3. These endothermic and exothermic peaks may also refer to several chemical and physical processes that occur as a result of thermal decomposition of Repag, Flu, Roben and Dano drugs at the temperature range given in Table 1.

3.3. Molecular orbital calculations (MO) of Repag, Flu, Roben and Dano drugs

MO calculation depending on the numbering system of Repag, Flu, Roben, and Dano drug molecules gives variable information about the structure of molecules both in neutral form (Fig. 4) and in charged form (Fig. 5), which actually are used to support the experimental evidence. The much important parameters calculated using MO calculation include bond orders, bond length and heat of formation.

3.4. Correlation between MS, TA Fragmentations and MO for charged molecular ions

The TGA of Repagdrug shows three main steps of decomposition. The first one occurs at 150–280 °C with an estimated weight loss = 17% due to the successive losses of CO_2 and C_2H_6 molecules (calcd. wt. loss = 16.37%). The inspection of MO calculation data (Table 2) revealed that this loss is due to the rupture of O50–H51 bond (bond order = 0.91337 and bond length = 0.96746) and C40–C48 bond (bond order = 0.93261 and bond length = 1.4737) to produce CO_2 molecule. The loss of C_6H_6 molecule is originated from the rupture of O50–H51 bond and C53–O52 bond (bond or-

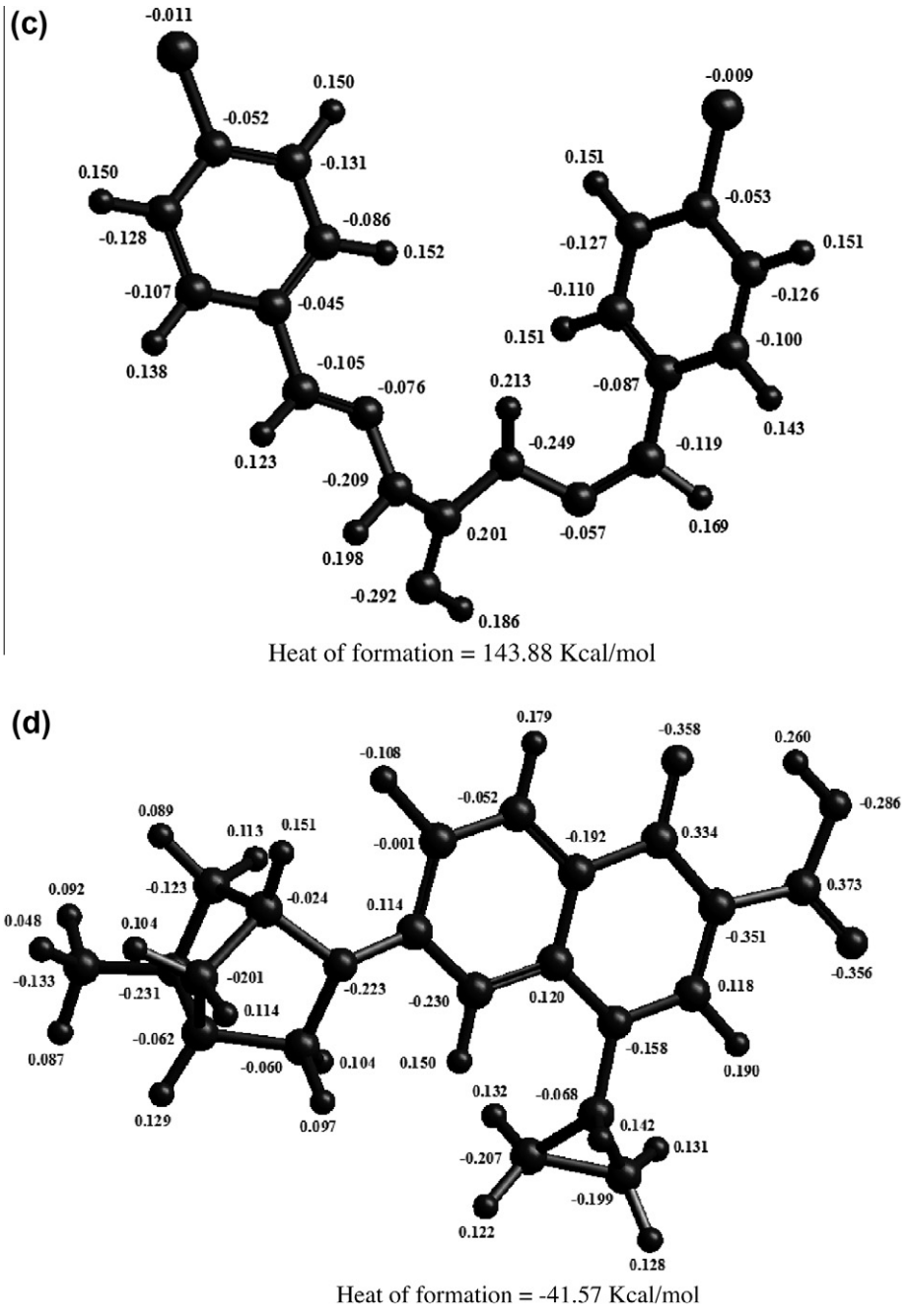

Figure 4 (*continued*)

der = 0.93458 and bond length = 1.4388). The appearance of fragment ion at m/z = 409 (RI = 100%) is due to the loss of CO_2 molecule obtained by rupture of O50–H51 and C40–C48 bonds.

This is followed by the second TA weight loss of $C_{22}H_{28}N_2O$ occurs at 280–390 °C of practical weight loss = 74.34% (calcd. wt. loss = 74.25%) as a result of rupture of the C27–N32 bond (bond order = 0.93812 and bond length = 1.4476), C40–C43 bond (bond order = 1.3147 and bond length = 1.4119) and C39–C42 bond (bond order = 1.4025 and bond length = 1.3975). The appearance of fragment ion at m/z = 172 (RI = 72%) may be accounted for the loss C_3H_5O obtained by rupture of C27–N32 and C27–H28 bonds.

According to the data listed in Table 1, the TGA of Flu drug shows three main steps of decomposition. The first one occurs at 100–275 °C of practical weight loss = 14.66% due to the loss of CO_2 molecule (calcd. wt. loss = 14.06%). The inspection of MO calculation data (Table 3) revealed that this loss is due to the rupture of O30–C31 bond (bond order = 0.93766 and bond length = 1.4336) and N26–C28 bond (bond order = 1.0387 and bond length = 1.3890). The appearance of fragment ion at m/z = 158 (RI = 27%) is due to the loss of CO molecule obtained by rupture of C28–N26 bond (Table 4).

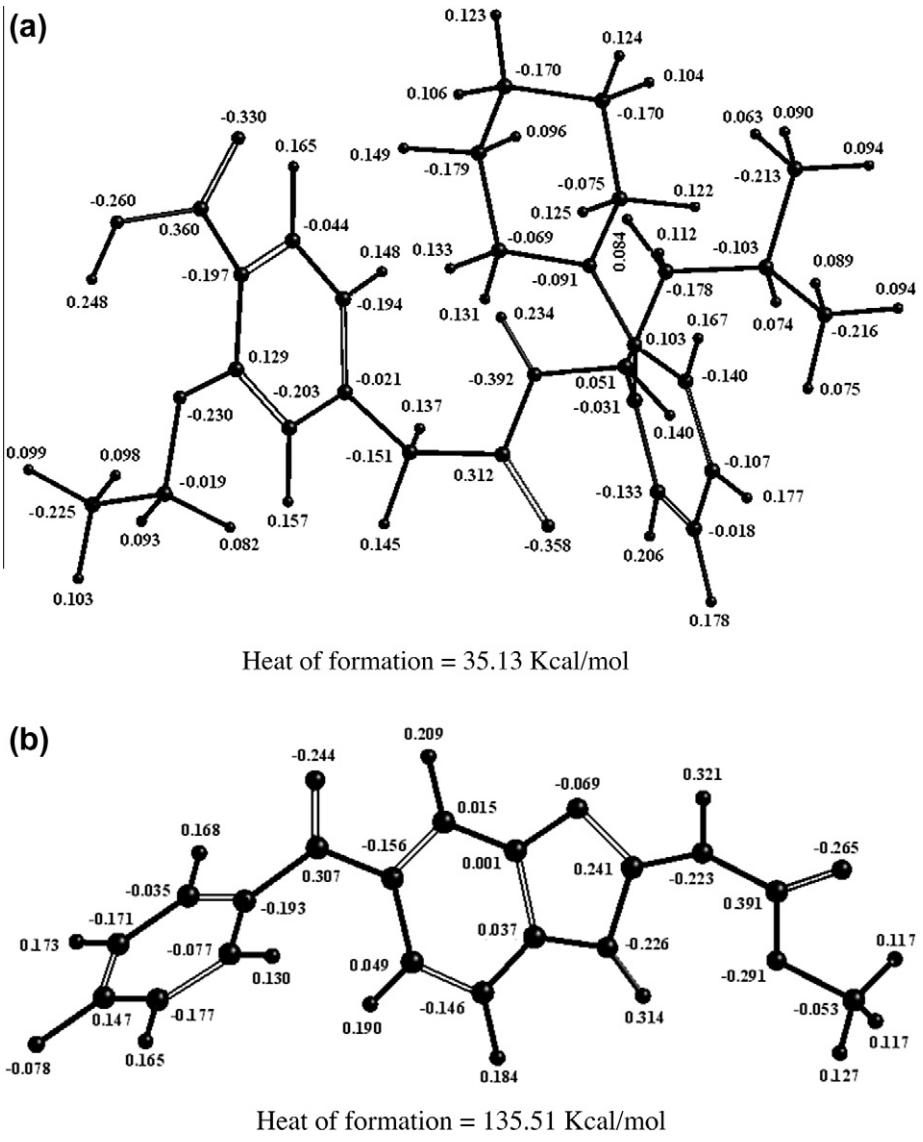

Figure 5 Charge distribution on different atoms for (a) Repag, (b) Flu, (c) Roben and (d) Dano charged molecular ions.

The third TA weight loss of $C_{13}H_8FN_2O$ occurs at 380–950 °C of practical weight loss = 72.31% (calcd. wt. loss = 72.52%) as a result of rupture of the following bonds: C7–C12 bond (bond order = 0.94172 and bond length = 1.4803), C12–C14 bond (bond order = 0.94344 and bond length = 1.4807), C15–N23 bond (bond order = 1.1184 and bond length = 1.396) and C19–N25 bond (bond order = 1.1643 and bond length = 1.4066). The appearance of fragment ion at m/z = 103 (RI = 11%) is due to the loss of $C_8H_6FN_3O$ obtained by rupture of C7–C12, C15–N23, and C19–N25 bonds. The appearance of fragment ion at m/z = 75 (RI = 39%) is due to the loss of CO molecule obtained by rupture of C12–C14 bond.

The TGA of Roben drug shows three steps of decomposition as given in Table 1. The first one occurs at 40–260 °C of practical weight loss = 9.79% due to the loss of HCl molecule (calcd. wt. loss = 9.85%). The appearance of fragment ion at m/z = 335 (RI = 41%) is due to the loss of HCl molecule.

This is followed by the second TA weight loss of $C_9H_8N_5Cl$ that occurs at 260–380 °C of practical weight loss = 59.93% (calcd. wt. loss = 59.76%) as a result of rupture of the following bonds: N14–C16 bond (bond order = 0.95435 and bond length = 1.4582), C16–N19 bond (bond order = 0.95816 and bond length = 1.4686), C4–C11 bond (bond order = 0.98565 and bond length = 1.4650), C22–C24 bond (bond order = 1.0078 and bond length = 1.4658), N13–N14 bond (bond order = 1.0563 and bond length = 1.3370), N21–C22 bond (bond order = 1.8231 and bond length = 1.3062), C11–N13 bond (bond order = 1.8405 and bond length = 1.2996) and C16–N18 bond (bond order = 1.8691 and bond length = 1.2969). The appearance of fragment ion at m/z = 154 (RI = 25%) is due to the loss of

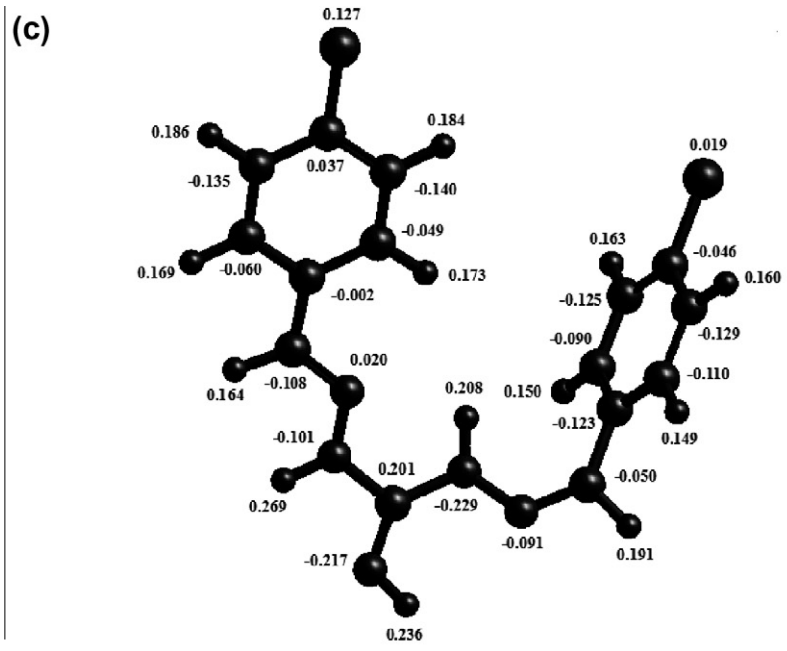

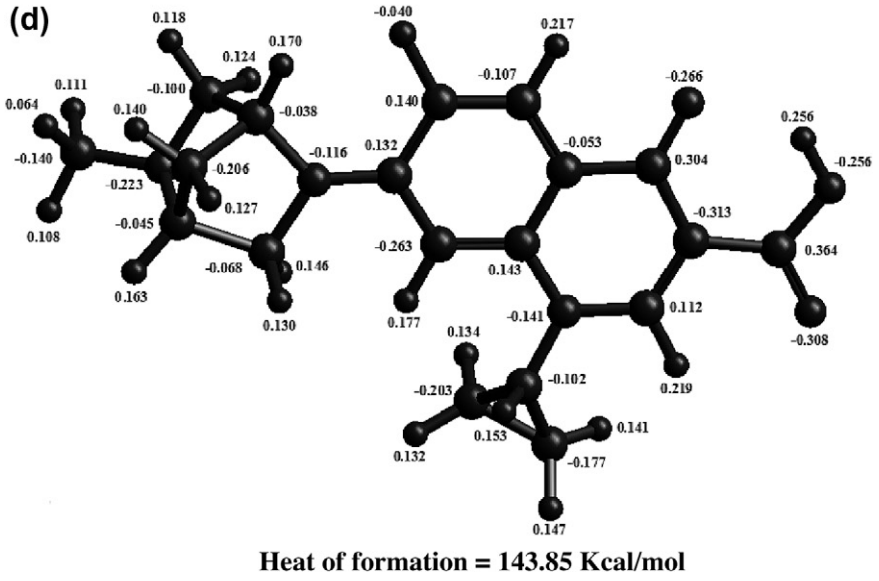

Figure 5 (*continued*)

CH_2N_2 obtained by rupture of C16–N19 bond. The appearance of fragment ion at m/z = 138 (RI = 47%) is due to the loss of $C_2H_4N_4$ obtained by rupture of N19–N21 bond (bond order = 1.3894 and bond length = 1.2735). The appearance of fragment ion at m/z = 125 (RI = 30%) is due to the loss of nitrogen atom obtained by rupture of N21–C21 bond (bond order = 1.3846 and bond length = 1.3605). The appearance of fragment ion at m/z = 75 (RI = 30%) is due to the loss of CHCl obtained by rupture of the following bonds: C25–Cl34 bond (bond order = 1.0865 and bond length = 1.6690) and C22–C24 bond (bond order = 1.2525 and bond length = 1.4170). The appearance of fragment ion at m/z = 85 (RI = 46%) is due to the loss of C_8H_6Cl obtained by rupture of N21–C22 bond and C11–N13 bond (bond order = 1.8565 and bond length = 1.2981) and C19–N25 bond. The appearance of fragment ion at m/z = 59 (RI = 100%) is due to the loss of N_2 molecule obtained by rupture of N13–N14 bond and N19–N21 bond.

The TGA of Dano drug shows that the first one occurs at 50–160 °C of practical weight loss = 4.08% due to the loss of CH_3 (calcd. wt. loss = 4.20%). The inspection of MO calculation data (Table 5) revealed that this loss is due to the rupture of N39–C40 bond (bond order = 0.98811 and bond length = 1.4409). The appearance of fragment ion at m/z = 276 (RI = 14%) is due to the loss of CH_3 and HF obtained by rupture of N39–C40, O16–H17 and C6–F26 bonds.

This is followed by the second TA weight loss of HF and C_6H_6NO occurs at 160–400 °C of practical weight

Table 2 Thermogravimetric data (TGA, DrTGA, and DTA) of Repag, Flu, Roben, and Dano drugs.

Drug	Temperature range (°C)	DrTGAmax (°C)	n^*	Mass loss % Found (Calcd.)	Assignment	DTA# (°C)
Repag	150–280	268	1	17.00 (16.37)	Loss of C_2H_6 and CO_2	152(+), 310(+), 358(−), 460(+), 540(−), 930(+).
	280–390	330	1	74.25 (74.34)	Loss of $C_{22}H_{28}N_2O$	
	390–1000	541, 938	2	9.40 (9.29)	Loss of C_2H_2O (complete decomposition)	
Flu	100–275	242	1	14.66 (14.06)	Loss of CO_2	242(+), 279(−), 333(+), 370(−), 513(+), 600(−), 689(−), 900(−).
	275–380	336	1	13.53 (13.42)	Loss of $CNHCH_3$	
	380–950	793	1	72.31 (72.52)	Loss of $C_{13}H_8FN_2O$ (complete decomposition)	
Roben	40–260	75	1	9.79 (9.85)	Loss of HCl	50(−), 84(+), 190(−), 271(+), 288(−), 313(+), 335 (−), 517(+), 580(+), 620(−), 663(−).
	260–380	290	1	59.93 (59.76)	Loss of $C_9H_8N_5Cl$	
	380–800	411, 657	2	31.02 (30.35)	Loss of C_6H_5Cl (complete decomposition)	
Dano	50–160	106	1	4.08 (4.20)	Loss of CH_3	115(+), 300(+), 337(+), 350(−), 423(+), 455(+), 594(−).
	160–400	344	1	35.35 (35.82)	Loss of C_6H_6NO and HF	
	400–500	467	1	12.35 (12.31)	Loss of CO_2	
	500–850	644	1	48.25 (47.57)	Loss of $C_{11}H_{10}N_2$ (complete decomposition)	

Table 3 Comparison of computed bond length in and bond order for Repag using AM1 method.

Bond	Bond order		Bond length		Bond	Bond order		Bond length	
	Neutral	Cation	Neutral	Cation		Neutral	Cation	Neutral	Cation
C1–C3	1.3784	1.1447	1.4126	1.4532	N32–C34	1.1307	1.0635	1.3751	1.3881
C1–C4	1.3658	1.1442	1.4127	1.4551	C34–O35	1.7298	1.7717	1.2496	1.245
C1–N11	0.97904	1.3124	1.4387	1.3617	C36–H37	0.94644	0.95164	1.1261	1.1243
C2–C5	1.3997	1.2717	1.3941	1.410	C36–H38	0.95921	0.94604	1.1221	1.1244
C2–C6	1.430	1.3712	1.3906	1.3956	C36–C39	0.98415	0.9853	1.4874	1.4879
C2–H10	0.94877	0.93723	1.0997	1.1031	C36–C34	0.91201	0.9127	1.5243	1.5227
C3–C6	1.388	1.4721	1.4022	1.3939	C39–C41	1.3802	1.3727	1.3999	1.4019
C3–C27	0.95023	0.93323	1.5171	1.5263	C39–C42	1.4025	1.4128	1.3975	1.3963
C4–C5	1.4352	1.5746	1.3893	1.3718	C40–C44	1.3804	1.3825	1.4008	1.3994
C4–H7	0.94751	0.9371	1.1018	1.1034	C40–C43	1.3147	1.3171	1.4119	1.4115
C5–H8	0.9486	0.93596	1.1001	1.1043	C40–C48	0.93261	0.92341	1.4737	1.4755
C6–H9	0.94583	0.92095	1.1023	1.1117	C41–C44	1.4302	1.4322	1.3908	1.3902
C12–C14	0.98851	0.98864	1.5135	1.5106	C41–H45	0.94662	0.94439	1.10	1.1008
C12–C16	0.97945	0.96558	1.5274	1.5312	C42–C43	1.3621	1.3488	1.4011	1.4034
C12–H17	0.96458	0.95528	1.1204	1.1223	C42–H46	0.93688	0.94061	1.1022	1.1002
C12–H22	0.96597	0.96176	1.1211	1.1224	C43–O52	1.0507	1.0632	1.3765	1.3733
C13–C14	0.98859	0.98899	1.5134	1.5116	C44–H47	0.9407	0.93961	1.1037	1.1037
C13–C15	0.97946	0.96964	1.5276	1.527	C48–O49	1.8078	1.794	1.2349	1.236
C13–H18	0.96368	0.94705	1.1205	1.1275	C48–O50	1.0558	1.0802	1.3625	1.3561
C13–H23	0.96668	0.9615	1.1211	1.1209	O50–H51	0.91337	0.91203	0.96746	0.96998
C14–H19	0.96614	0.95786	1.1207	1.1225	C53–O52	0.93458	0.92841	1.4388	1.4411
C14–H24	0.96648	0.96289	1.1219	1.1225	C53–H54	0.95381	0.95454	1.1214	1.1214
C15–N11	0.95869	0.91077	1.4622	1.4529	C53–H55	0.95356	0.95388	1.1217	1.1214
C15–H20	0.95757	0.94704	1.1262	1.1207	C53–C56	0.99001	0.98958	1.5107	1.5102
C15–H25	0.9534	0.9263	1.1297	1.1371	C56–H57	0.97304	0.97243	1.1164	1.1164
C16–N11	0.95941	0.91756	1.4625	1.4584	C56–H58	0.96842	0.96585	1.1161	1.1166
C16–H21	0.95637	0.95344	1.1266	1.1276	C56–H59	0.97374	0.97237	1.1162	1.1165
C16–H26	0.9532	0.93593	1.130	1.1311	C60–H61	0.95529	0.95556	1.1283	1.1281
C27–C29	0.95741	0.96315	1.5421	1.5372	C60–C62	0.98852	0.98739	1.5148	1.515
C27–H28	0.94305	0.93412	1.1383	1.1445	C60–C66	0.98819	0.98692	1.5155	1.5163
C27–N32	0.93812	0.94625	1.4476	1.443	C62–H63	0.97565	0.97368	1.1168	1.117
C29–C60	0.97536	0.97361	1.5228	1.5228	C62–H64	0.97443	0.97415	1.1166	1.1162
C29–H30	0.96272	0.96213	1.1201	1.1202	C62–H65	0.97599	0.97348	1.1167	1.1174
C29–H31	0.96475	0.96088	1.1223	1.1248	C66-H67	0.9758	0.97537	1.117	1.1168
N32–H33	0.8890	0.8887	0.99287	0.99468	C66–H68	0.97576	0.97322	1.1165	1.117
					C66–H69	0.97592	0.97301	1.1166	1.116

Table 4 Comparison of computed bond length in and bond order for Flu using AM1 method.

Bond	Bond order		Bond length		Bond	Bond order		Bond length	
	Neutral	Cation	Neutral	Cation		Neutral	Cation	Neutral	Cation
H1–C2	0.94409	0.93894	1.0995	1.1013	C16–H20	0.93783	0.92379	1.1017	1.1063
C2–C4	1.4362	1.4404	1.3901	1.3897	C16–C19	1.3035	1.1138	1.4002	1.4328
C2–C5	1.3555	1.3514	1.4079	1.4087	C17–C18	1.5019	1.3780	1.3859	1.4008
C3–H10	0.94338	0.94686	1.1023	1.1014	C17–H21	0.94456	0.93146	1.1023	1.1073
C3–C6	1.4367	1.4565	1.3906	1.3881	C18–H22	0.94543	0.93361	1.0980	1.1023
C3–C7	1.3773	1.3544	1.3997	1.4017	C19–N25	1.1643	1.5024	1.4066	1.3502
C4–C7	1.3754	1.3624	1.4019	1.4038	N23–H35	0.87078	0.84717	0.98868	0.9962
C4–H8	0.94177	0.93894	1.1029	1.1040	N23–C24	1.1010	1.15820	1.4291	1.4150
C5–F11	1.0238	1.0437	1.3532	1.3490	C24–N25	1.5552	1.15370	1.3671	1.4407
C5–C6	1.3545	1.3354	1.4080	1.4111	C24–N26	1.0166	1.2482	1.4070	1.3619
C6–H9	0.94458	0.94134	1.0994	1.1005	N26–H27	0.8731	0.85004	1.0027	1.0126
C7–C12	0.94172	0.96355	1.4803	1.4691	N26–C28	1.0387	0.92043	1.3890	1.4173
C12–O13	1.3829	1.9117	1.2387	1.2349	C28–O29	1.7205	1.8100	1.2397	1.2298
C12–C14	0.94344	0.9008	1.4807	1.4967	C28–O30	0.99963	1.0325	1.3787	1.3659
C14–C16	1.4520	1.5750	1.3946	1.3785	O30–C31	0.93766	0.90351	1.4336	1.4456
C14–C17	1.3029	1.2297	1.4110	1.4215	C31–H32	0.96357	0.96188	1.1163	1.1163
C15–C18	1.2892	1.0559	1.4002	1.4937	C31–H33	0.95647	0.95179	1.1181	1.1186
C15–C19	1.2563	1.1055	1.4529	1.3961	C31–H34	0.96360	0.96188	1.1162	1.1163
C15–N23	1.1184	1.4107	1.3960	1.3843					

Table 5 Comparison of computed bond length in and bond order for Roben using AM1 method.

Bond	Bond order		Bond length		Bond	Bond order		Bond length	
	Neutral	Cation	Neutral	Cation		Neutral	Cation	Neutral	Cation
H1–C2	0.94368	0.94385	1.1015	1.1015	C16–N19	0.95816	0.87639	1.4686	1.4806
C2–C4	1.3855	1.3795	1.3999	1.400	N18–H17	0.92873	0.90396	0.99636	0.99971
C2–C5	1.4209	1.4256	1.3941	1.3936	N19–H20	0.89828	0.85205	1.0158	1.0202
C3–C6	1.3776	1.3751	1.3995	1.4005	N19–N21	1.0582	1.3894	1.3399	1.2735
C3–C7	1.4358	1.4377	1.3917	1.3916	N21–C22	1.8231	1.3846	1.3062	1.3605
C3–H10	0.94441	0.94128	1.1007	1.1018	C22–H23	0.92867	0.92437	1.1134	1.1148
C4–C7	1.3741	1.3705	1.4020	1.4023	C22–C24	1.0078	1.2525	1.4658	1.4170
C4–C11	0.98565	0.98872	1.4650	1.4645	C24–C26	1.3806	1.2107	1.4006	1.4254
C5–C6	1.3911	1.3861	1.3978	1.3991	C24–C27	1.3662	1.2010	1.4039	1.4297
C5–H8	0.94444	0.94202	1.1008	1.1016	C25–Cl34	1.0006	1.0865	1.6991	1.6690
C6–Cl35	1.0009	1.0118	1.6990	1.6941	C25–C28	1.3766	1.2746	1.3994	1.4149
C7–H9	0.94629	0.94443	1.1009	1.1016	C25–C29	1.3894	1.2815	1.3976	1.4139
C11–H12	0.92016	0.91180	1.1097	1.1132	C26–C29	1.4228	1.5380	1.3938	1.3790
C11–N13	1.8405	1.8565	1.2996	1.2981	C26–H30	0.94379	0.93787	1.1011	1.1035
N13–N14	1.0563	1.0142	1.3370	1.3504	C27–C28	1.4384	1.5481	1.3913	1.3772
N14–H15	0.89066	0.89110	1.0112	1.0111	C27–H31	0.94688	0.9385	1.1009	1.1039
N14–C16	0.95435	0.99109	1.4582	1.444	C28–H32	0.94471	0.93398	1.1006	1.1049
C16–N18	1.8691	1.8805	1.2969	1.2939	C29–H33	0.94471	0.93477	1.1007	1.1047

loss = 35.35% (calcd. wt. loss = 35.82%) as a result of rupture of the following bonds: O16–H17 bond (bond order = 0.89602 and bond length = 0.97059), N9–C18 bond (bond order = 0.92795 and bond length = 1.4346), C7–C13 bond (bond order = 0.97739 and bond length = 1.4716), C6–F26 bond (bond order = 1.0045 and bond length = 1.3578) and C4–N9 bond (bond order = 1.0287 and bond length = 1.4092). The appearance of fragment ion at m/z = 313 (RI = 13%) is due to the loss of CO_2 obtained by rupture of O16–H17 and C12–C14 bonds.

This is followed by the third TA weight loss of CO_2 molecule occurs at 400–500 °C of practical weight loss = 12.35% (calcd. wt. loss = 12.31%) as a result of rupture of C12–C14 bond (bond order = 0.94881 and bond = 1.4688). The appearance of fragment ion at m/z = 313 (RI = 13%) is due to the loss of CO_2 obtained by rupture of O16–H17 and C12–C14 bonds.

This is followed by the fourth TA weight loss of $C_{11}H_{10}N_2$ occurs at 500–850 °C of practical weight loss = 48.25% (calcd. wt. loss = 47.57%) as a result of rupture of the following bonds: N28–C34 bond (bond order = 0.9354 and bond length = 1.4804), N28–C29 bond (bond order = 0.93714 and bond length = 1.4825), C34–C36 bond (bond order = 0.94929 and bond length = 1.580), C29–C32 bond (bond order = 0.95973 and bond length = 1.5676), C32–C44 bond (bond order = 0.96029 and bond length = 1.5785),

Table 6 Comparison of computed bond length in and bond order for Dano using AM1 method.

Bond	Bond order		Bond length		Bond	Bond order		Bond length	
	Neutral	Cation	Neutral	Cation		Neutral	Cation	Neutral	Cation
H1–C2	0.94111	0.93294	1.1029	1.1052	C19–H22	0.95552	0.95523	1.1057	1.1055
C2–C4	1.3409	1.4266	1.4089	1.3969	C19–H23	0.95674	0.95522	1.1054	1.1058
C2–C5	1.3716	1.2261	1.4117	1.4304	C20–H24	0.95625	0.95275	1.1051	1.1065
C3–H8	0.93426	0.91983	1.1053	1.1110	C20–H25	0.95767	0.95203	1.1049	1.1069
C3–C6	1.4372	1.3816	1.3944	1.400	O27–C13	1.7756	1.8330	1.2462	1.2404
C3–C7	1.3363	1.4144	1.3984	1.3880	N28–C29	0.93714	0.90623	1.4825	1.4787
C4–C7	1.3147	1.1490	1.4164	1.4447	N28–C34	0.9354	0.89311	1.4804	1.4816
C4–N9	1.0287	1.1131	1.4092	1.3926	C29–H30	0.95259	0.93828	1.1203	1.1229
C5–C6	1.2297	1.0683	1.4363	1.4696	C29–H31	0.95259	0.93759	1.1205	1.1229
C5–N28	1.0907	1.3471	1.3962	1.3453	C29–C32	0.95973	0.95571	1.5785	1.5803
C6–F26	1.0045	1.0730	1.3578	1.3392	C32–H33	0.9449	0.93549	1.1076	1.1098
C7–C13	0.97739	0.93702	1.4716	1.4870	C32–N39	0.96674	0.97216	1.4873	1.4833
N9–C10	1.1858	1.1190	1.3689	1.3815	C32–C44	0.96029	0.95583	1.5676	1.5681
N9–C18	0.92795	0.91314	1.4346	1.4390	C34–H35	0.93719	0.93158	1.1086	1.1095
C10–H11	0.92134	0.91039	1.1136	1.1167	C34–C36	0.94929	0.93352	1.5800	1.5878
C10–C12	1.5719	1.6342	1.3784	1.3725	C34–C44	0.97057	0.96239	1.5699	1.5708
C12–C13	1.0079	1.0064	1.4568	1.4539	C36–H37	0.95242	0.94819	1.1198	1.1223
C12–C14	0.94881	0.91716	1.4688	1.4788	C36–H38	0.95709	0.94934	1.1205	1.1195
C14–O15	1.7663	1.8016	1.2399	1.2357	C36–N39	0.96788	0.97184	1.4836	1.4807
C14–O16	1.0772	1.0872	1.3570	1.3530	N39–C40	0.98811	0.97485	1.4409	1.4422
O16–H17	0.89602	0.90145	0.97059	0.96963	C40–H41	0.96567	0.96252	1.1218	1.1225
C18–C19	0.97076	0.95866	1.5165	1.5195	C40–H42	0.95952	0.96093	1.1248	1.1241
C18–H21	0.93338	0.93015	1.1161	1.1164	C40–H43	0.9664	0.96332	1.1216	1.1221
C18–C20	0.96362	0.96663	1.5187	1.5176	C44–H45	0.96167	0.95872	1.1098	1.1105
C19–C20	0.99084	0.99283	1.4973	1.4963	C44–H46	0.96135	0.95285	1.1105	1.1127

Table 7 Thermodynamic parameters of the thermal degradation of Repag, Flu, Roben, and Dano drugs.

Drug	Temperature range (°C)	Thermodynamic parameters				
		E^* (kJ mol^{-1}) HM (CR)	A (S^{-1}) HM (CR)	ΔS^*(kJ mol^{-1} k^{-1}) HM(CR)	ΔH^*(kJ mol^{-1}) HM(CR)	ΔG^*(kJ mol^{-1}) HM(CR)
Repag	210–280	211.8 (180.8)	2.47 × 1020 (7.45 × 1016)	140.6 (73.14)	207.3 (176.3)	131.3 (136.7)
	280–390	97.47 (89.24)	8.95 × 107 (7.34 × 106)	−98.55 (−119.3)	92.46 (84.23)	151.9 (156.2)
	470–602	53.28 (40.83)	2.54 × 102 (5.19 × 101)	−207.3 (−220.5)	46.51 (34.06)	215.2 (213.5)
	915–970	176.9 (116.3)	6.20 × 106 (2.33 × 104)	−126.6 (−173.0)	166.8 (106.2)	320.1 (315.7)
Flu	198–274	217.9 (204.3)	1.2 × 1022 (9.5 × 1019)	173.5 (133.0)	213.6 (200.0)	124.2 (131.5)
	274–378	88 (79)	1.0 × 107 (1.2 × 106)	−116.7 (−134.3)	83.0 (73.9)	154.0 (155.7)
	378–950	56.6 (44.5)	3.5 × 101 (4.5 × 103)	−225.9 (−185.6)	47.0 (35.7)	288.5 (233.5)
Roben	40–110	11.3 (6.0)	5.35 (1.58)	−232.4 (−242.5)	8.4 (3.1)	89.96 (88.22)
	233–380	66.8 (60.9)	3.96 × 105 (1.79 × 104)	−143.1 (−168.8)	62.08 (56.24)	142.6 (151.3)
	380–480	61.8 (52.4)	8.35 × 103 (1.29 × 103)	−176.8 (−192.3)	56.12 (46.74)	177.0 (178.3)
	480–700	9.9 (6.4)	5.0 × 10–2 (5.6 × 10–2)	−279.3 (−297.5)	2.20 (1.38)	262.0 (275.3)
Dano	50–150	104.8 (98.47)	2.43 × 1014 (6.88 × 1012)	−28.50 (−11.46)	101.6 (95.31)	90.83 (95.75)
	278–415	102.8 (95.10)	1.63 × 108 (7.81 × 106)	−93.75 (−119.0)	97.65 (89.96)	155.5 (143.4)
	415–508	49.28 (34.96)	3.26 × 102 (2.18 × 10)	−204.4 (−226.9)	43.12 (28.80)	194.4 (196.7)
	508–765	49.91 (30.48)	4.98 × 101 (1.60)	−221.8 (−250.4)	42.29 (22.85)	245.7 (252.5)

C32–N39 bond (bond order = 0.96674 and bond length = 1.4873), C36–N39 bond (bond order = 0.96788 and bond length = 1.4836), C34–C44 bond (bond order = 0.97057 and bond length = 1.5699) and C5–N28 bond (bond order = 1.0907 and bond length = 1.3962). The appearance of fragment ion at m/z = 82 (RI = 100%) is due to the loss of $C_{12}H_8N_2O$ obtained by rupture of N28–C34 and N28–C29 bonds. The appearance of fragment ion at m/z = 70 (RI = 22%) is due to the loss of CH_2 obtained by rupture of C32–C44 bond and C34–C44 bonds.

3.5. Kinetic and thermodynamic studies

The thermodynamic activation parameters of decomposition processes of REPAG, FLU, ROBEN and DANO namely activation energy (E^*), enthalpy (ΔH^*), entropy (ΔS^*) and Gibbs free energy change of the decomposition (ΔG^*) were evaluated graphically by employing the Coats–Redfern and Horowitz–Metzger relations (Leversen, 1978; Somogyi et al., 1991) The data are summarized in Table 6. The entropy of activation (ΔS^*), enthalpy of activation (ΔH^*) and the free energy change

of activation (ΔG^*) were calculated using the following equations (Table 7):

$$\Delta S^* = 2.303[\log(Ah/kT)]R \quad (1)$$

$$\Delta H^* = E^* - RT \quad (2)$$

$$\Delta G^* = \Delta H^* - T\Delta S^* \quad (3)$$

As regards, the stability of the investigated drugs during their thermal degradation, the stability increases with the increase in the activation energy needed for their thermal decomposition reactions. The activation energy (kJ mol^{-1}) of the first decomposition step of Flu, Repag, Dano and Roben drugs, respectively, using HM and CR methods decreases in the following order (Zayed et al., 2007):

$$217.9(204.3) > 211.8(180.8) > 104.8(98.47) > 11.3(6.0)$$

It can be concluded that, the thermal stability of the investigated drugs decreases in the following order: Flu > Repag > Dano > Roben.

4. Conclusion

It is important to make a comparative discussion between results of TA and MS of Repag, Flu, Roben, and Dano drugs. This comparison shows the agreement and disagreement between the two techniques used in studying the drug fragmentation pathways. Therefore, the best fragmentation pathway of this drug is correctly selected. In both TA and MS techniques there is an agreement and it finally concluded that, it is highly effective to use TA, MS and MO in one team to explain efficiently the best fragmentation pathway of Repag, Flu, Roben, and Dano drug molecules.

Acknowledgements

The authors extend their appreciation to the Deanship of Scientific Research at King Saud University for funding the work through the research group project No. RGP-VPP-007.

References

Bourcier, S., Hoppilliard, Y., 2003. Eur. J. Mass Spectrom. 9, 351–360.
Coats, A.W., Redfern, J.P., 1964. Nature 201, 68–69.
Dewar, M.J., Zoebisch, E.G., Healy, E.F., Stewart, J.J.P., 1985. J. Am. Chem. Soc. 107, 3902–3909.
Fahmey, M.A., Zayed, M.A., El-Shoubaky, H.G., 2005. J. Therm. Anal. Calor. 82, 137.
Horowitz, H.H., Metzegar, G., 1963. Anal. Chem. 35, 1464–1468.
Kerns, E.H., Rourich, R.A., Volk, K.J., Lee, M.S., 1997. J. Chromatogr. B 698, 133–145.
Larsen, B.S., Me Ewen, C.N., 1998. Mass Spectrometry of Biological Materials, Marcel Dekker, New York, (Eds.).
Leversen, K., 1978. Fundamental Aspects of Organic Mass Spectrometry. Verlag Chemie, Weinheim, New York.
Somogyi, A., Gomory, A., Tamas, K.V., 1991. J. Org. Mass Spectrom. 26, 936–938.
Zayed, M.A., Fahmey, M.A., Hawash, M.A., El-Habeeb, A.A., 2007. Spectrochimica Acta (Part A) 67, 522–530.